Indian Journal of Radio & Space Physics
Vol. 12, February 1983, pp. 13-17

Fine Sun Sensor for APPLE Satellite

M P PHILIP & Y K JAIN
Sensors Section, ISRO Satellite Centre, Bangalore 560 058

Received 2 *April* 1982; *revised received* 31 *July* 1982

A miniature precision fine sensor used in APPLE, the first Indian geostationary satellite, for sun acquisition and for fine pointing of the satellite roll-axis towards the sun, has been developed. This sensor uses a quadrant photodiode and an aperture mask for generating the two-axis error signals. The linear field range is ± 20 and the null accuracy is better than 0.25 . The null accuracy can be improved by reducing the linear field.

1 Introduction

A miniature sun sensor of high accuracy, stability and ruggedness in construction was developed and used in APPLE spacecraft for sun acquisition and for fine pointing of the satellite roll-axis towards the sun. This sensor, called the fine sun sensor (FSS), provided outputs over a linear range of $\pm 20^{\circ}$ for pitch and yaw loop control during sun acquisition and is the first of the type developed for 3-axis stabilized satellites. The sensor uses a quadrant photodiode detector and an aperture mask for the measurement. The whole sensor weighs 75 gm. The overall field-of-view about each axis is $\pm 50^{\circ}$ and null accuracy is better than 0.25°. The null accuracy can be improved with a corresponding reduction in the linear field.

2 Principle of Operation

The sun beam is directed to the appropriate detector by an aperture mask. The aperture mask is etched on a small quartz plate coated with chromium. The aperture plate with the quadrant photodiode, called the optical assembly (Fig. 1) is the principal part of the FSS. Radiation from the sun passing through the aperture casts an image of the aperture on the detectors. The pitch and yaw detectors are so arranged that an energy balance is obtained on the detectors when the sensor is pointed towards the centre of the sun. Fig. 2 shows the typical pitch or yaw output signal over the entire field of view. The process by which the aperture generates the two-axis linear error signals, and the illumination pattern of the detector area for different sun angles are shown in Fig. 3. It is to be noted that the radiation distribution does not change the shape, but does change the position with respect to the aperture.

When the sensor is aligned with the sun as shown in Fig. 3(b), equal areas of the detectors are illuminated and the sensor output is nulled. When the sensor is misaligned with sun as shown in Fig. 3(a) and (c), one detector is illuminated more than the other and the difference in illumination area is a measure of the output signal. For a square aperture of length L, placed at a distance H from the detector, the difference in area of illumination is given as $LH \tan\theta$, where θ is the misalignment angle. So for small values of θ, the output increases linearly with this misalignment angle (neglecting the cosine effect). The linear field angle φ is given as $\varphi = \tan^{-1}(L/2H)$. The gain of the amplifier is so designed that the amplifier saturates at $\varphi = \tan^{-1}(L/2H) = 20^{\circ}$ and the condition is shown in Fig. 3(d).

A highly reflective optical surface (alignment mirror) fixed to sensor housing defines the null axis of the sensor and is used for sensor alignment. Since the

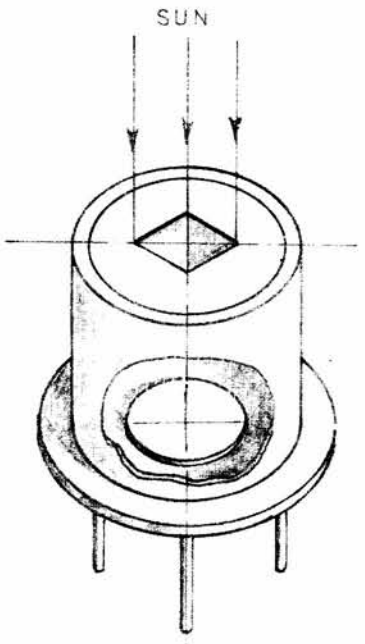

Fig. 1—Optical assembly FSS

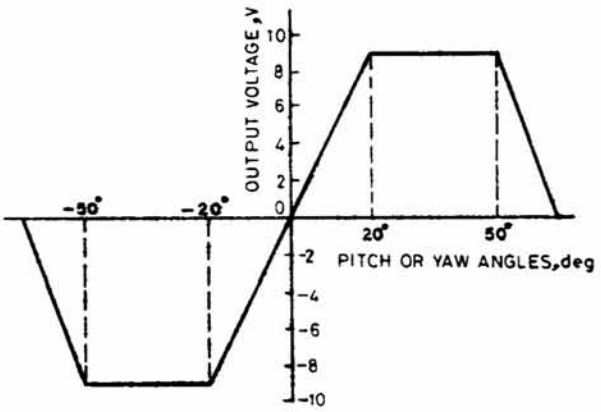

Fig. 2—Typical response function of FSS

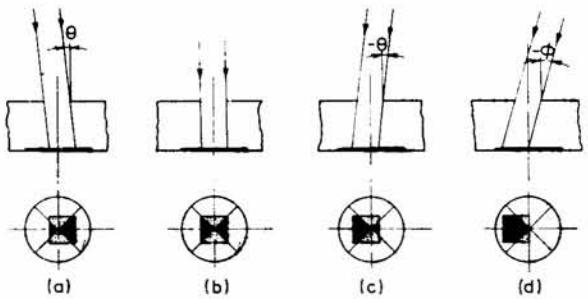

Fig. 3—Detector illumination scheme for different sun angles

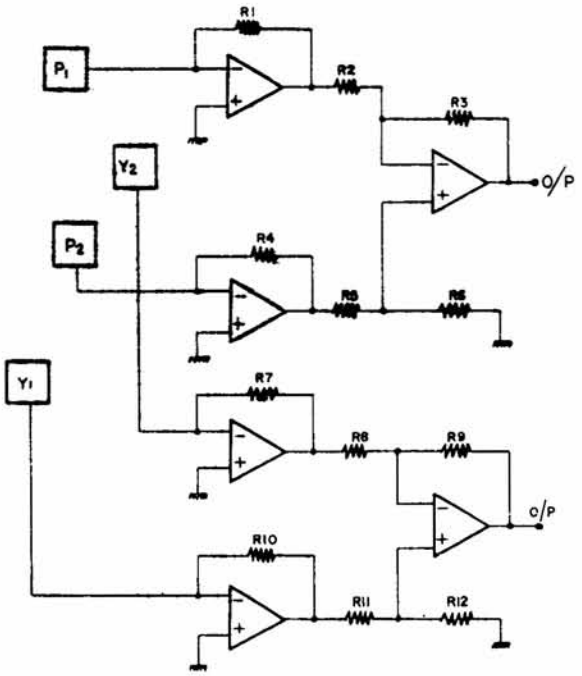

Fig. 4—Electrical configuration of FSS

optical assembly is highly rigid, there is no possibility of any relative movement between detector and aperture and a highly repeatable transfer function is achieved.

3 Description of the Sensor Assembly

The sensor consists of (i) a mechanical housing, (ii) optical assembly, (iii) electronics block, and (iv) alignment mirror. The mechanical housing includes the basic housing and the special mounting arrangements of the optical, electronics and alignment subassemblies.

The electrical configuration is shown in Fig. 4. A current amplifier converts the short circuit current of each detector into a voltage function proportional to the illuminated area of the detector. These voltage functions are connected in differential mode to derive the pitch and yaw outputs. Bias voltages to electrically nullify the pitch and yaw channels, test inputs to check the channels and voltage regulators for amplifier supplies are also provided for better accuracy.

An isometric view of the sensor is shown in Fig. 5. The optical block forms the principal part of the sensor. The aperture plate is a thin circular quartz plate of diameter 20 mm and thickness 0.5 mm, one surface of which is coated with chromium. A rectangular aperture of 3 × 3 mm is etched centrally on this plate by precision chemical etching of the chromium coating. The detector is a quadrant photodiode of Centronic

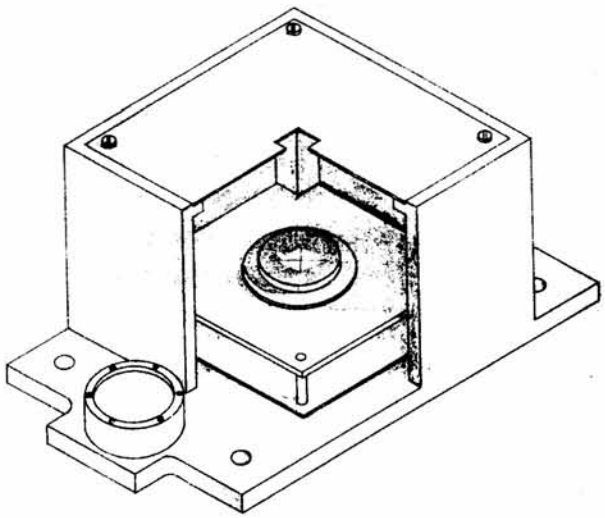

Fig. 5—Fine sun sensor

make type No. QD-100 with an active area diameter of 11 mm and qualifying the MIL specifications. The circular sensitive flake area is divided into four equal sections and is positioned 2.3 mm below the optical window. The aperture plate is cemented to the optical window with the chromium coated surface in contact with the optical window with transparent optical cement.

Before cementing, the aperture plate is aligned concentric with the circular sensitive flake and with the diagonals of the aperture window in line with the line

of separation of the detectors. This critical alignment is done using a precision microscope. This unit forms the optical block and all critical geometric relationships are established when the aperture is cemented to the detector. This detector assembly with aperture, is mounted on a printed circuit board, which in turn is firmly fixed to the main housing by four screws. The electronics assembly contains the printed circuit board of the amplifiers and processing circuits. The detectors are operated in zero bias configuration and the short circuit current of each photodiode is converted to a voltage function by separate current amplifiers.

The alignment assembly consists of a circular glass plate of diameter 15 mm polished to $\lambda/4$. The polished surface is coated with a highly reflective coating and is used as the optical reference surface. This glass plate is mounted rigidly in a small aluminium housing between two O rings of RTV and forms the alignment assembly. This assembly is mounted on the base flange of the sensor main housing with a ball and three screws arrangement. Two-axis tilting of the reference plane is possible by adjusting the 3 screws, thereby enabling the reference plane normal to be exactly aligned with the null axis of the sensor. This alignment is done using an autocollimator.

4 Sensor Alignment and Calibration

The pitch and yaw error electrical signals derived from the sensor represent the optical axis offset from the centre of illumination of the sun disc. The errors which degrade this measurement are (i) the alignment error, (ii) the drift errors due to environment, and (iii) the noise errors.

The alignment error is a fixed error and is caused by the inaccuracies in aligning the optical axis of the sensor with the centre of illumination of the solar disc. This alignment is very critical and is done using an autocollimator. First, the autocollimator is mounted in front of the sun simulator and its axis is aligned to the centre of the sun disc. The specifications of the sun simulator and autocollimator are presented in Table 1. In between the simulator and autocollimator the sensor is mounted on a two-axis turntable as shown in Fig. 6. The sensor is now pointed towards the simulator so that the pitch and yaw electrical outputs are zero. This corresponds to the electrical null of sensor. In this condition the alignment mirror normal should point exactly towards the centre of the solar disc. To check this, the sensor is rotated exactly through 180° around one of its axis, either pitch or yaw. In the new position the alignment mirror normal should coincide with the autocollimator axis. If it is not coincident, tilt the mirror assembly accordingly and repeat the process till alignment mirror normal at electrical null of the sensor is in line with the autocollimator axis aligned to the sun disc. Thus the alignment error depends on how well the sun line can be established with the autocollimator and how accurately it can be transferred to the sensor reference mirror and the electrical null axis of the sensor.

Table 1—Specifications of Sun Simulator and Autocollimator

Sun simulator	
Sun beam diameter	80 mm
Light source	Xenon arc lamp
Intensity	Variable from 0.5 to 1 solar constant
Beam divergence	30 arc min
Autocollimator	
Angular range	16 arc min
Resolution	0.1 arc sec

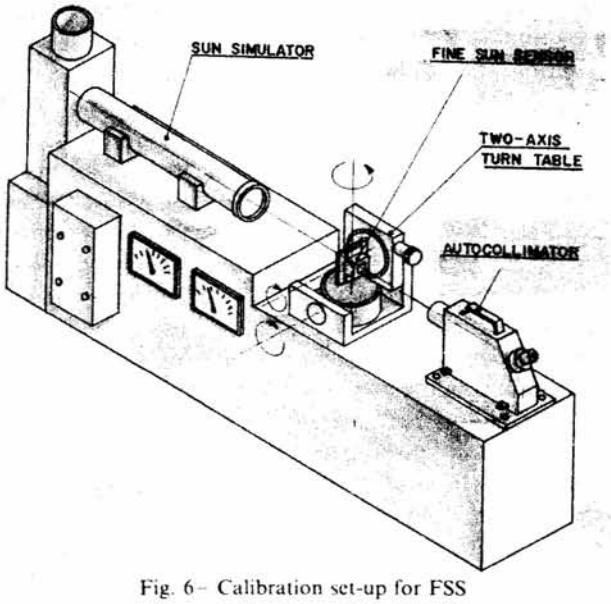

Fig. 6— Calibration set-up for FSS

The drift error is defined as the angular change between the mounting plane of the sensor and its electrical null due to environmental variations inducing electrical and mechanical instabilities in the detector and the other associated elements. The uneven heating or cooling can cause expansion and shifting of the aperture with respect to the detector. By using low coefficient of expansion materials this error can be made negligible. The amount of drift caused by the detector responsivity variation due to differential temperature between detector pairs can be calculated. The electronic and detector noise is another source of error to be experimentally determined and accounted for.

After identifying the null axis of the sensor, the sensor is rotated around the pitch and for different values of pitch error, the output voltage is noted. The

measurement is repeated by introducing a known amount of yaw error on the sensor thus taking measurements for various values of cross misalignment. Next, the rotations are carried out around yaw axis for different values of pitch error and the sensor output is noted. Thus the sensor is calibrated for yaw and pitch outputs by using the solar simulator. Due compensation is applied for the simulated solar constant of the source in the calibration curve.

5 Flight Performance in APPLE Satellite

For the sun pointing of the roll-axis of the satellite, it was originally planned to use the 4π sensor output for initial acquisition from any random orientation and then transfer the controls to the FSS outputs for fine pointing. But the acquisition sequence had to be modified due to the non-deployment of the north panel. Due to constraints in the envelope of the satellite, 4π sensors were mounted in four locations under the solar panels. So the non-deployment of one panel puts severe constraint on the performance of 4π sun sensor and thus on the sun acquisition sequence. So the acquisition was carried out by actuating the pitch/yaw acquisition logic taking inputs from the FSS. In the modified acquisition sequence, the satellite was put in spin mode with spin axis oriented normal to the sun line and then despun to 0.5 rpm. The outputs of the FSS was monitored and the yaw control loop was switched on as soon as the yaw output was available from the sensor. Once the yaw loop was established, the pitch loop was initiated. This technique worked and sun acquisition to satellite roll-axis was established. Figs 7 and 8 show the outputs of the sun sensor during the sun acquisition period, showing how the pitch and yaw errors of the satellite were developing during the period and the arrows indicate the points at which the thrusters fired automatically to correct the satellite pitch and yaw errors. It can be seen that the thrusters kept the satellite roll-axis oriented towards the sun within $\pm 6^{\circ}$.

After the earth acquisition of the satellite, the outputs of the FSS were monitored on a continuous basis which enabled us to analyse and evaluate the sensor performance. In the 3-axis stabilized condition, as the satellite local time changes, the sun position with respect to the sensor also changes and very accurate

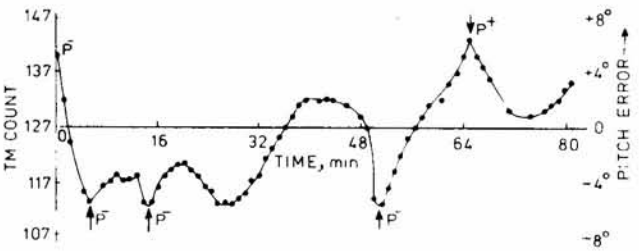

Fig. 7—Curve showing the nature of pitch control from FSS (The sun tracking mode operation of APPLE on 23 June 1981 is shown from 20 10 33 to 21 30 32 hrs. P^+ denotes positive pitch thruster firing and P negative pitch thruster firing.)

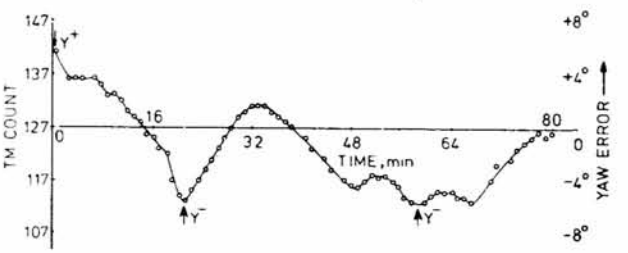

Fig. 8—Curve showing the nature of yaw control from FSS (Sun tracking was done on 23 June 1981 from 21 10 33 to 20 30 32 hrs. Y^+ indicates positive yaw thruster firing and Y negative yaw thruster firing.)

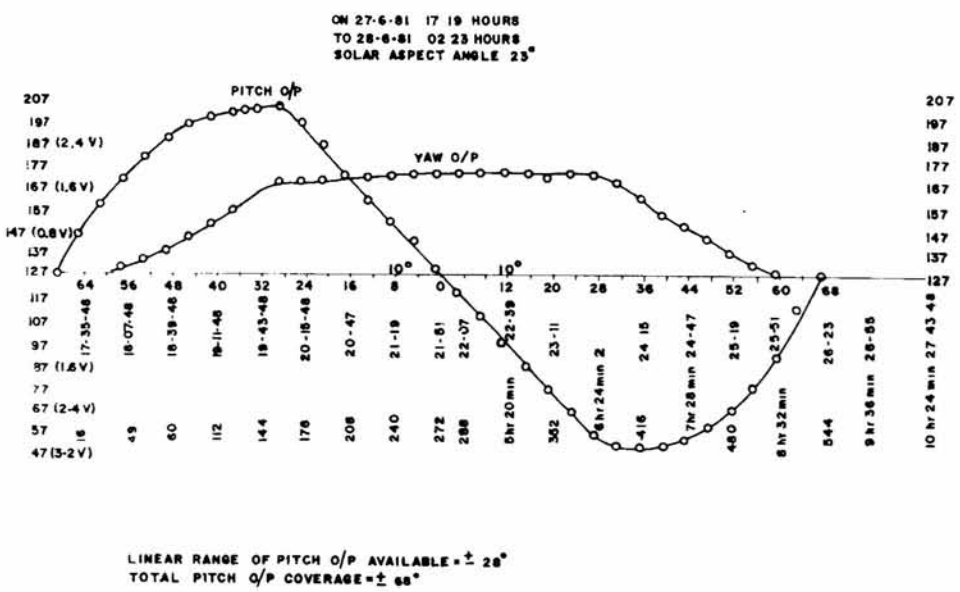

Fig. 9—Pitch and yaw outputs of FSS

measurement of pitch output with respect to sun position is possible. This pitch response curve of the sensor is shown in Fig. 9. The field-of-view and the slope of the sensor response curves tallied very well with the ground simulated results. Again, the off-axis accuracies are very good and the calculations of signal amplitude depending upon the solar constant, declination etc. by extrapolation of the ground facility, have been fully validated. Interestingly, this sensor was also used for measuring the longitude of the satellite during station-keeping manoeuvres, since the zero-pitch output of the sensor indicates 6 AM satellite local time which is directly a measurement of satellite longitude. By modifying the mask shape and distance, the field-of-view can be narrowed and accuracy can be improved. The advantage of using a quadrant photodiode lies in the fact that the matching of the four photodiodes is very good, noise equivalent power (NEP) is very low and variation of responsivity with temperature etc. is uniform, thereby providing better accuracy.

Acknowledgement

The authors are grateful to Prof. U R Rao, Director, ISRO Satellite Centre, Bangalore, for the encouragement given for the development of the sensor. They are also thankful to Mr R M Vasagam, Project Director, APPLE, for his guidance and help in this work.

NATIONAL SCIENCE LIBRARY
16/046
27.4.04
NEW DELHI